

Inhomogeneous magnetoelectric coupling in $\text{Pb}(\text{Zr}, \text{Ti})\text{O}_3/\text{Terfenol-D}$ laminate composite

Jian-ping Zhou^{*}, Ling Meng, Ze-hu Xia, Peng Liu, and Gang Liu

Citation: *Appl. Phys. Lett.* **92**, 062903 (2008); doi: 10.1063/1.2841660

View online: <http://dx.doi.org/10.1063/1.2841660>

View Table of Contents: <http://aip.scitation.org/toc/apl/92/6>

Published by the [American Institute of Physics](#)



**THE WORLD'S RESOURCE FOR
VARIABLE TEMPERATURE
SOLID STATE CHARACTERIZATION**



OPTICAL STUDIES SYSTEMS



SEEBECK STUDIES SYSTEMS



MICROPROBE STATIONS



HALL EFFECT STUDY SYSTEMS AND MAGNETS



WWW.MMR-TECH.COM

Inhomogeneous magnetoelectric coupling in Pb(Zr,Ti)O₃/Terfenol-D laminate composite

Jian-ping Zhou,^{1,a)} Ling Meng,¹ Ze-hu Xia,¹ Peng Liu,¹ and Gang Liu²

¹School of Physics and Information Technology, Shaanxi Normal University, Xi'an 710062,

People's Republic of China

²State Key Laboratory for Mechanical Behavior of Materials, School of Material Science and Engineering, Xi'an Jiaotong University, Xi'an 710049, People's Republic of China

(Received 7 November 2007; accepted 18 January 2008; published online 11 February 2008)

Inhomogeneous magnetoelectric coupling in a simple Pb(Zr,Ti)O₃/Terfenol-D laminate composite is investigated. Four magnetic-field-induced voltage (MIV) and three electric-field-induced magnetization (EIM) resonance frequencies are caused by magnetomechanical and electromechanical resonances. The different positions in the sample have different contributions to the MIV and EIM, which are mainly related to the resonant behaviors and the corresponding strain distribution. The MIV distribution shows mirror symmetry, while the EIM distribution shows mirror antisymmetry. The EIM with different directions forms close electric-field-induced magnetic loops around Terfenol-D to meet the lowest magnetic energy. These results are helpful for the future design of magnetoelectric devices. © 2008 American Institute of Physics.

[DOI: 10.1063/1.2841660]

Multiferroic materials have drawn an increasing stimulating interest because of their attractive multifunctionality.^{1,2} These materials combine ferroelectric/antiferroelectric and ferromagnetic/antiferromagnetic orders, between which some effects can be produced, such as the magnetoelectric (ME) or magnetodielectric effect.^{1,2} ME materials can generate an electric polarization in an external magnetic field or a magnetic response to an applied electric field. Recently, a great deal of studies on the ME effect in single phases and composites have been reported. The ME effect in single phases is weak and commonly appears at low temperature.^{2,3} Alternatively, piezoelectric/magnetostrictive composites enjoy a stronger effective stress-mediated ME coupling resulting from the product property at room temperature. Recently, giant ME effect has been found in composites containing Pb(Zr,Ti)O₃ (PZT) with high piezoelectric constant,⁴⁻⁷ Terfenol-D,^{6,8} FeBSiC,⁹ giant magnetostrictive alloys, especially in the laminate composites.^{4,6,8,9}

Up to now, most studies on the ME effect have focused on magnetic-field-induced electric polarization in an external magnetic field, whereas investigations on magnetic response to an applied electric field have been seriously absent. There have only been several experimental and theoretical reports about electric-field-induced magnetization (EIM) in recent years.^{7,10-12} This is an unproportionate phenomenon in the active multiferroic research field. Moreover, ME coupling was usually characterized from the whole surfaces of samples.^{4-6,8,9} Thus, the contribution of the different positions in the sample to the ME coupling is unclear, especially at the resonance frequency. In this letter, we investigate the ME coupling characteristics in a simple laminate structure. The EIM and magnetic-field-induced voltage (MIV) distributions in the sample are studied, especially at the resonance frequency.

Terfenol-D and PZT were selected as the magnetostrictive and piezoelectric components for their excellent magnetostrictive and piezoelectric properties. The PZT component was polarized in the thickness direction, and Terfenol-D was magnetized along the longitudinal direction. Terfenol-D and PZT tablets with the same diameter of 20 mm were bonded together by epoxy bonder. The thicknesses of the PZT and Terfenol-D tablets were set to 1.5 and 3.5 mm, respectively, because ME coupling is stronger at this ratio in consideration of the loss.¹³ We deposited gold on the PZT surface as an electrode to perform the MIV and EIM measurements. Then we polished the gold and deposited gold dots 1 mm in diameter to investigate the MIV distribution. The MIV was measured by using a dynamic method with a small ac magnetic sine signal δH_{ac} superimposed on a dc magnetic field H_{bias} as done previously,^{4,6} both of which were along the x direction, as shown by the inset in Fig. 1(b). $H_{bias}=600$ Oe was adopted for the largest MIV values at this static magnetic field. We measured the induced charge Q with a charge amplifier connected to an oscilloscope and obtained the voltage values with the relationship $\delta V_{ac}=Q/C$, where C is the capacitance. The MIV coefficient was calculated with $\alpha_V=\delta V_{ac}/\delta H_{ac}$. The EIM measurement was performed in a reverse way.¹¹ The laminate sample was placed in a dc bias magnetic field, as shown by the inset in Fig. 3. When applying a sine electric field δE_{ac} on PZT, the induced strain in PZT was acoustically transferred to Terfenol-D; as a result, an induced magnetization δM_{ac} in Terfenol-D was produced due to magnetoelastic coupling. The EIM in Terfenol-D was measured by using a search coil, which was connected to an amplifier, then an oscillograph. The EIM coefficient was expressed by $\alpha_M=\delta M_{ac}/\delta E_{ac}$.

Figure 1(a) shows the MIV dependence on frequency at $H_{bias}=600$ Oe. Four MIV resonant peaks are observed. The first one at 23 kHz is attributed to the magnetomechanical resonance (MMR) mainly relative to Terfenol-D. According to the literature, ME resonance is caused by electromechanical resonance (EMR).^{4,6,14,15} In fact, MMR can also result in

^{a)} Author to whom correspondence should be addressed. Electronic mail: zhoujp@snnu.edu.cn.

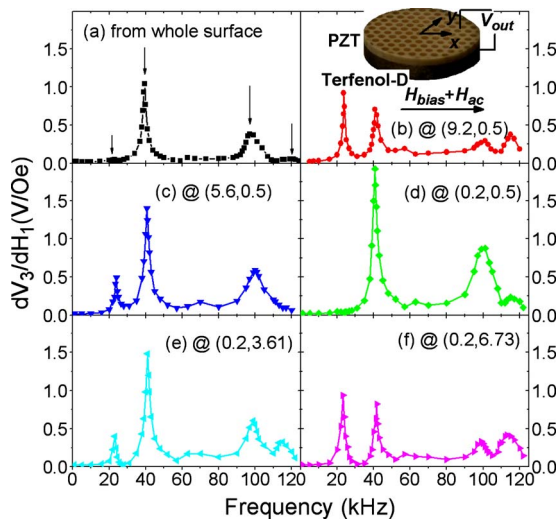


FIG. 1. (Color online) The MIV coefficients as functions of the frequency for the laminate composite. The data are collected from (a) the whole surface of the composite and from the dot at $(x,y)=(b) (9.2,0.5)$, (c) $(5.6,0.5)$, (d) $(0.2,0.5)$, (e) $(0.2,3.61)$, and (f) $(0.2,6.73)$, the unit of which is millimeter. The inset shows the schematic illustration of the laminate composite used for measuring the MIV distribution.

ME resonance. The detailed information will be published elsewhere. The other three peaks are relative to the EMR and are the first-order flexural resonance mode, the second-order flexural resonance mode, and the radial resonance mode, respectively.^{6,14} In order to reveal the mechanism of these resonance modes, we investigated the distribution of the MIV response on the surface of PZT. Parts of the spectra at different positions are shown in Figs. 1(b)–1(f). In comparison with the whole surface, shown in Fig. 1(a), some places have higher contribution to ME coupling, while some places have lower contribution, especially at the resonance frequency. The ME coefficient from the whole surface can be regarded as the average from the different positions. The different MIV resonant values at the different positions are relative to the different ME resonant mechanisms. The MIV coefficients at the resonance frequency are summed in Fig. 2, where the position parameters are illuminated by the inset in Fig. 1(b), presuming the center as the origin. The MIV coefficients at 16 kHz (amplified ten times), the nonresonant MIVs, are also plotted for comparison. Under an applied H_{bias} and δH_{ac} along the x direction, a symmetric ac elastic strain will be excited about the centerline at $x=0$ of the Terfenol-D layer via magnetoelastic coupling. The strain transfers to the PZT layer, producing electric polarization with the same symmetry by the piezoelectric effect.⁸ The MIV reveals different characteristics at the different resonance modes. The two flexural resonance MIVs have similar behaviors, with the largest center value decreasing gradually to the edge value, shown like an umbrella in Fig. 2(d), which combines these three figures. This is caused by the electro-mechanical flexural resonance, which shares similar oscillational behaviors with the MIV distribution in bilayered composites.¹⁴ The MIV at 115 kHz, being relative to the electromechanical radial resonance, increases along the x and y axes from the center to the edge and presents lower values at other positions, as shown in Figs. 2(a)–2(c) and 2(e). The centerline of the composite at $x=0$ is located on a stress concentration line, and the two ends are located at stress-free points.⁸ The large MIVs will be produced at these positions.

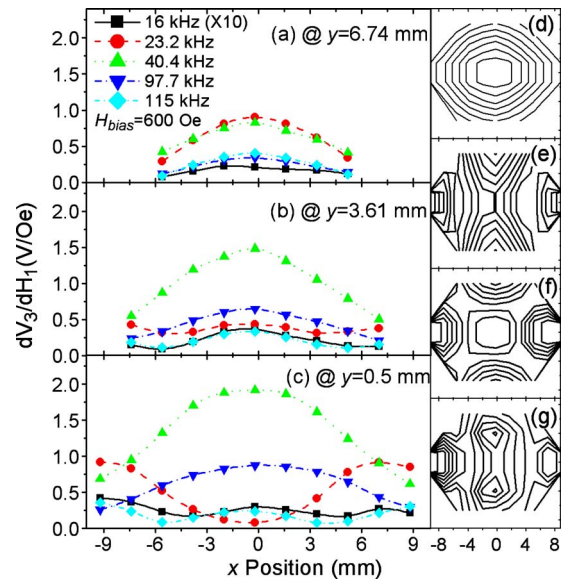


FIG. 2. (Color online) (a)–(c) are the MIV distributions at the MIV resonance frequency as well as at 16 kHz. The MIV data at 16 kHz are amplified ten times. (d)–(f) are the contour figures at 41, 113, 23.2, and 16 kHz, respectively.

The MM resonant and nonresonant MIVs share the same characteristics. They show strong ME coupling at the centerline and near the two edges, as shown in Figs. 2(f) and 2(g). The Terfenol-D layer shows MMR at a given frequency of 23.2 kHz, resulting in a large strain. The strain transfers to the PZT layer, producing electric polarization. Because the resonance is from the Terfenol-D layer and not from the PZT layer, the MIV at 23.2 kHz shares the same characteristics with that at the nonresonance frequency, but with large values.

We then investigated the EIM in Terfenol-D with a search coil under the sine electric field δE_{ac} of about 2.7×10^4 V/m and the bias magnetic field $H_{\text{bias}}=150$ Oe, referring to the literature.¹¹ Figure 3 shows the EIM coefficients at $(x,y)=(5.5 \text{ mm}, 0 \text{ mm})$ on the Terfenol-D surface as a function of frequency. When the driving electric field is near the EMR frequency, three maximum EIM values reach 18.3, 7.0, and 3.9 mA/V. This indicates that the EIM effect depends significantly on the driving electric field frequency. The three resonance frequencies in the electrical impedance are 38, 89, and 112 kHz for the sample, but the MIV resonance frequencies increase, whereas the EIM resonance fre-

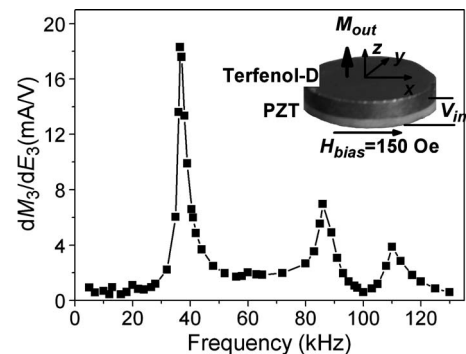


FIG. 3. The EIM coefficients obtained at $(x,y)=(5.5 \text{ mm}, 0 \text{ mm})$ on the Terfenol-D surface as a function of the frequency under $H_{\text{bias}}=150$ Oe. The inset shows the schematic illustration of the laminate composite used for the EIM measurements.

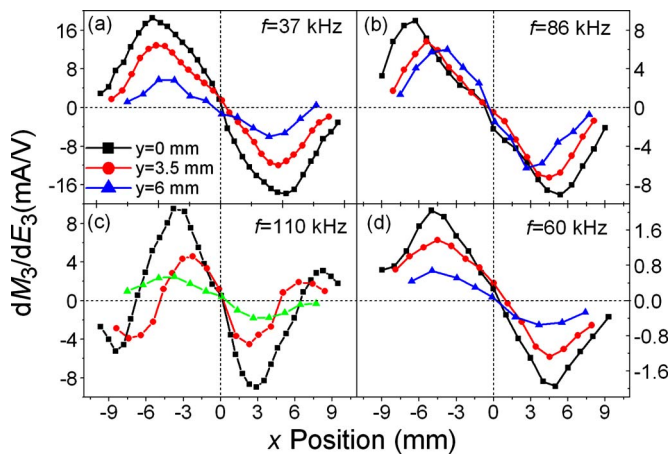


FIG. 4. (Color online) The EIM distribution on the Terfenol-D surface at three EIM resonance frequencies and a nonresonance frequency.

quencies decrease. When putting Terfenol-D into the dc magnetic field, the MIV resonance frequencies occur redshifted, considering the loss,¹³ while the EIM resonance frequencies occur blueshifted reversely.

The EIM distribution on the Terfenol-D surface was subsequently investigated at the above condition. Figure 4 shows the EIM distribution at three resonance frequencies together with a nonresonance frequency of 60 kHz. The EIM distributions at the flexural resonance frequencies and at the nonresonance frequency share the same characteristics; i.e., the EIM value increases to a maximum and then reduces from the y axis to both sides of the sample. The large EIM values appear like two waning moons on the surface of Terfenol-D. The EIM changes directions twice at 110 kHz, which should be attributed to the radial resonance mode. The EIM distribution presents mirror antisymmetry about the yz plane, absolutely different from the mirror symmetry of the MIV distribution. The MIV shows the same sign because the PZT component was polarized along the z direction. Terfenol-D was magnetized along the x direction, but the EIM was measured in the z direction. The opposite EIM directions out of plane at $x < 0$ and $x = 0$ would bring magnetic loops. Then, we measured the EIM in the x direction at (0, 0, and 1.5 mm), where the position parameters are illuminated by the inset in Fig. 3, and obtained 9.0, 5.1, 3.2, and 0.95 mA/V for 37, 86, 110, and 60 kHz, respectively. The EIM loops around Terfenol-D are helpful in reducing magnetic energy.

MIV and EIM are two converse methods for describing ME materials. They can be characterized by one parameter, $\alpha = (\partial P / \partial H)_E = \mu_0 (\partial M / \partial E)_H$.¹⁰ However, the MIV and EIM values are different at the different positions in the sample,

resulting in difficulty to compare them. We calculated them with the largest value for the sample at the first-order flexural resonance frequency. It is $\alpha = 3.5 \times 10^{-8}$ s/m for the EIM collected at $f = 37$ kHz and $H_{\text{bias}} = 500$ Oe, at which the largest EIM value appears, and is $\alpha = 1.01 \times 10^{-7}$ s/m for the MIV data. The two values are close. The lower value for EIM may be caused by the noncontact measurement and the fact that the component EIM values are obtained only in the z direction.

In summary, four MIV and three EIM resonance frequencies are found and attributed to the MMR and EMR modes. The latter modes play a dominating role in ME coupling. The ME parameters obtained from the two converse measuring methods are close. The different positions in the sample have different contributions to the MIV and EIM, especially at the resonance frequencies, attributed to the different resonance modes and the corresponding strain distribution. The MIV distribution exhibits mirror symmetry about the yz plane, while the EIM distribution shows mirror antisymmetry, forming magnetic loops around Terfenol-D to reduce magnetic energy. The results are helpful for the future design of ME devices.

This work was supported by the National Natural Science Foundation of China (Grant Nos. 50772065 and 50572059). The authors thank Professor C. W. Nan and Dr. J. Ma for help in the ME measurements.

¹W. Eerenstein, N. D. Mathur, and J. F. Scott, *Nature (London)* **442**, 759 (2006).

²M. Fiebig, *J. Phys. D* **38**, R123 (2005).

³W. Prellier, M. P. Singh, and P. Murugavel, *J. Phys.: Condens. Matter* **17**, R803 (2005).

⁴J.-p. Zhou, H.-c. He, Z. Shi, G. Liu, and C.-W. Nan, *J. Appl. Phys.* **100**, 094106 (2006).

⁵G. Srinivasan, E. T. Rasmussen, and R. Hayes, *Phys. Rev. B* **67**, 014418 (2003).

⁶Z. Shi, J. Ma, Y. Lin, and C.-W. Nan, *J. Appl. Phys.* **101**, 043902 (2007).

⁷M. Gomi, N. Nishimura, and T. Yokota, *J. Appl. Phys.* **101**, 09M109 (2007).

⁸S. Dong, J. Zhai, F. Bei, J. F. Li, and D. Viehland, *Appl. Phys. Lett.* **87**, 062502 (2005).

⁹S. Dong, J. Zhai, Z. Xing, J. Li, and D. Viehland, *Appl. Phys. Lett.* **91**, 022915 (2007); S. Dong, J. Zhai, J. Li, and D. Viehland, *ibid.* **89**, 252904 (2006).

¹⁰W. Eerenstein, M. Wiora, J. L. Prieto, J. F. Scott, and N. D. Mathur, *Nat. Mater.* **6**, 348 (2007).

¹¹J. G. Wan, J.-M. Liu, G. H. Wang, and C. W. Nan, *Appl. Phys. Lett.* **88**, 182502 (2006).

¹²L. Li and J. Y. Li, *Phys. Rev. B* **73**, 184416 (2006).

¹³F. Yang, Y.-M. Wen, P. Li, M. Zheng, and L.-X. Bian, *Acta Phys. Sin.* **56**, 3539 (2007) (in Chinese).

¹⁴Z. Shi, Ph. D. thesis, Tsinghua University, 2006.

¹⁵J. G. Wan, Z. Y. Li, Y. Wang, M. Zeng, G. H. Wang, and J.-M. Liu, *Appl. Phys. Lett.* **86**, 202504 (2005).